THE ASTROPHYSICAL JOURNAL, 350:767–775, 1990 February 20

PHOTOMETRIC AND POLARIMETRIC VARIABILITY AND MASS-LOSS RATE OF THE MASSIVE BINARY WOLF-RAYET STAR HDE 311884 (WN6+O5: V)[1]

ANTHONY F. J. MOFFAT, LAURENT DRISSEN,[2] CARMELLE ROBERT,[3] ROBERT LAMONTAGNE,[4] ROGER COZIOL, AND NORMAND MOUSSEAU
Département de physique, Université de Montréal
VIRPI S. NIEMELA[5,6] AND MIGUEL A. CERRUTI[5,7]
Instituto de Astronomia y Fisica del Espacio, Buenos Aires
WILHELM SEGGEWISS
Observatorium Hoher List, Universität Bonn
AND
NIELS VAN WEEREN
Leiden Observatory
Received 1989 April 7; accepted 1989 August 19

ABSTRACT

Photometric and polarimetric monitoring of the Wolf-Rayet (W-R)+O-type binary system HDE 311884 = WR 47 over many orbital cycles shows the clear effects of phase-dependent electron scattering of O-star light as the orbiting O companion shines through varying column density of W-R stellar wind material. In contrast to this wind-type eclipse, the stars themselves do not quite eclipse. Both photometry and polarimetry give a consistent estimate of the mass-loss rate of the W-R component: $\dot{M} \cong 3 \times 10^{-5}\ M_\odot\ \mathrm{yr}^{-1}$. The orbital inclination, $i \cong 70°$, along with the previously published velocity orbit, yields high masses: $M(\mathrm{WN6}) \cong 48\ M_\odot$ and $M(\mathrm{O5{:}\ V}) \cong 57\ M_\odot$.

Subject headings: polarization — stars: eclipsing binaries — stars: individual (HDE 311884) — stars: mass loss — stars: Wolf-Rayet

I. INTRODUCTION

With spectral type WN6+O5: V, the double-line, SB2 binary HDE 311884 (=WR 47 in the catalog of van der Hucht *et al.* 1981) contains the most massive W-R star known with any reliability. Niemela, Conti, and Massey (1980; hereafter NCM) determined minimum masses ($M \sin^3 i$) of 40 $M_\odot$ for the WN6 component and 47 $M_\odot$ for the O star. A more recent determination (Niemela and Mandrini 1989; hereafter NM) yields similar values with an improved ephemeris (W-R star in front at JD 2,443,918.4 + $6^{\mathrm{d}}.239\ E$).

A high mass for the WN6 (possibly even WN7: cf Lamontagne and Moffat 1987) star is not surprising in the Conti scenario (Conti 1976) in which WNL stars (=WN6, 7, 8, 9; L = late) resemble most their O-type cousins, the Of stars. Other binary systems with WNL stars (mostly SB1) may also have high masses (cf. Smith and Maeder 1989), but none of these is as reliably observed as HDE 311884. Hotter WN stars (WNE = WN2, 3, 4, 5; E = early) are generally less luminous (Lundström and Stenholm 1984), have broader emission lines, and are less massive (Moffat 1981, 1982). Also, the mass ratio of WR 47 is relatively high ($Q = M_{\mathrm{W\text{-}R}}/M_{\mathrm{O}} \approx 0.83$: cf. NCM) compared to WNE and WC binaries ($Q \sim 0.2$–0.5: cf. Moffat 1981, 1982).

Determination of the actual masses of the components requires knowledge of the orbital inclination, i. In principle, the value of i can be extracted in several ways: (*a*) by assuming a mass for one of the stars based on its spectral type, (*b*) from an analysis of the light curve, or (*c*) from phase-dependent linear polarization modulation.

The first method is interesting only if all else fails, e.g. one assumes a mass for the O star, calculates i, and then deduces $M_{\mathrm{W\text{-}R}}$. In the case of WR 47, the spectral type of the O star is not well known.

The second method requires a sufficiently high value of i to yield eclipses, either mutually involving the stars themselves or from the phase-dependent diminution of the light from one star as it orbits in the wind of the other star. A preliminary study of the light curve of WR 47 (Cerruti 1984; and more intensively by Lamontagne and Moffat 1987) shows a relatively noisy light curve, typical of WNL stars, with a $\sim$0.1 mag dip near phase zero (using the revised NM ephemeris) when the W-R star is on the near side of its orbit. This suggests a wind-type eclipse of the O star as it orbits in the W-R star wind.

The third method is useful even for low inclinations and has been used very successfully for many W-R+O binaries (cf. St-Louis *et al.* 1988). A preliminary study of WR 47 in polarization by Moffat and Seggewiss (1987) yielded $i = 77°$ on the basis of only six data points.

The purpose of this paper is to elaborate on methods (*b*) and (*c*) on the basis of extensive data sets. Averaging over many

[1] Based partly on observations collected at the European Southern Observatory (ESO), Chile.

[2] Visiting Astronomer, Cerro Tololo Inter-American Observatory (CTIO), National Optical Astronomical Observatory, operated by the Association of Universities for Research in Astronomy, Inc., under contract with the National Science Foundation.

[3] Visiting Astronomer, South African Astronomical Observatory, Sutherland Station.

[4] Visiting Astronomer, University of Toronto southern telescope, Las Campanas, Chile.

[5] Visiting Astronomer, Complejo Astronomico El Leoncito, San Juan, Argentina.

[6] Member of Carrera del Investigador, CIC, Prov. Buenos Aires, Argentina.

[7] Member of Carrera del Investigador, CONICET, Argentina.

cycles should help tie down the mean light curve. In polarization it is probably better first to treat each epoch of data independently (cf. Dolan and Tapia 1988). This should yield a more secure value of the orbital inclination, the masses, and the mass-loss rate of the W-R component.

II. OBSERVATIONS

Table 1 lists the six currently available photometric data sets and the four polarimetric sets. Note that the SAAO data include simultaneous photometry and linear and circular polarimetry.

Table 2 gives the journal of observations of the new photometric data. The photometry refers to magnitude differences straight from the telescope without allowance for atmospheric extinction or reference to standard stars; the only adjustment made was a constant added to the magnitudes of each data set for normalization, so that $m(0.25 < \phi < 0.75) \approx$ constant for each set. The most numerous 1987 CTIO data were used as a reference. The symmetric pattern of data taking (e.g., sky–C2–C3–W-R–C3–C2–sky) in all cases eliminates linear drifts in instrumental sensitivity and atmospheric extinction. The total time spent obtaining one data point was typically 15 minutes. Note that the Walraven data (magnitudes and colors) are given in *magnitude* differences, not the usual log intensity units.

Table 3 presents the linear and circular polarization data. Columns (3) to (8) give, respectively, the degree of linear polarization P and its mean error σ_p; the position angle θ of linear polarization in the equatorial frame and its mean error σ_θ; and the degree of circular polarization V and its mean error σ_v.

Light curves are presented in Figures 1–3. Figure 1 shows a plot of the magnitudes of WR 47 minus comparison star versus the NM phase for each of the 1987 sets of photometry. Figure 2 shows the Walraven color indices plotted as for the light curves in Figure 1. Figure 3 depicts the 1987 V-data differences in magnitude for the two comparison stars, C3 − C2, versus phase for the variable star C3 (cf. Lamontagne and Moffat 1987). The overall scatter in Figure 3 ($\sigma_{o-c} \simeq 0.004$ mag) indicates the instrumental precision of a typical data point.

Figure 4 gives a plot of the linear polarization parameters P, θ, versus phase for each data set. (The fitted curves will be discussed below.) Note the difference $\Delta\theta \sim 1^\circ.5$ between the two sets of V data; this likely reflects the level of *systematic* errors that prevails here. Figure 5 shows a phase plot of the circular polarization data, contemporaneous with the linear SAAO data at the top of Figure 4.

III. ANALYSIS AND DISCUSSION

a) Photometry

All magnitude light curves obtained after 1984 (cf. Fig. 1 and Lamontagne and Moffat 1987) show the same trend: a

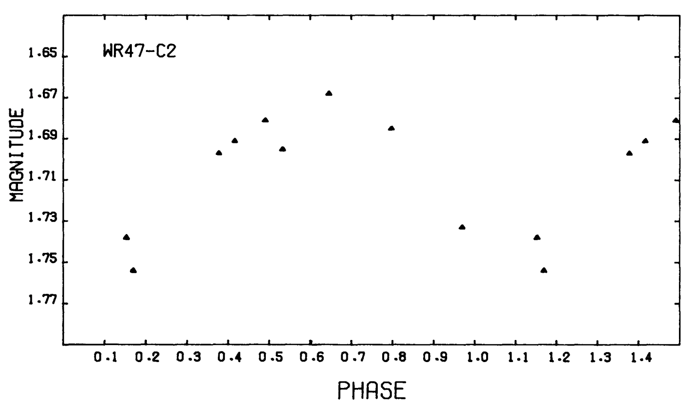

FIG. 1*a*

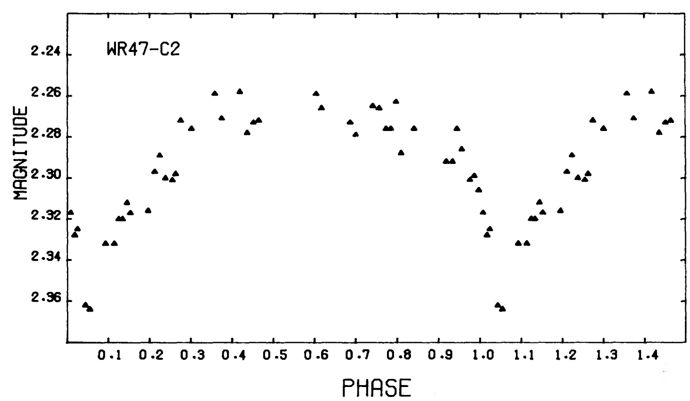

FIG. 1*b*

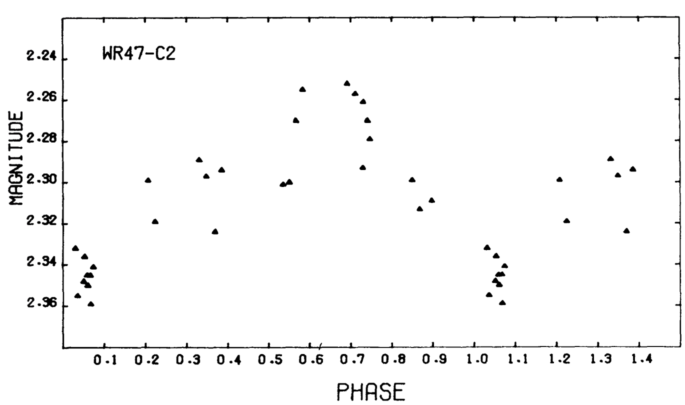

FIG. 1*c*

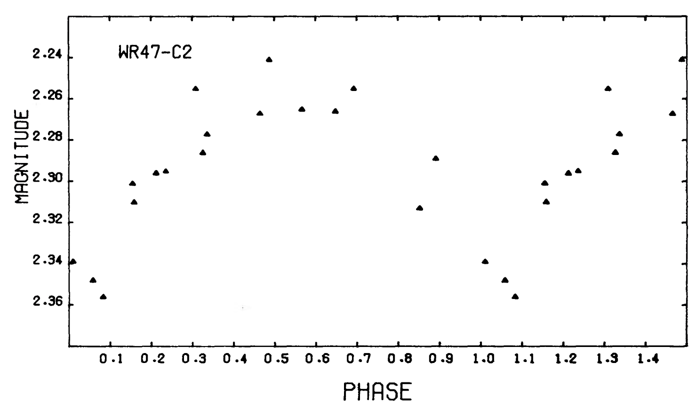

FIG. 1*d*

FIG. 1.—The 1987 light curves of WR 47–C2 (cf. Table A), phased according to NM. (*a*) SAAO in R; (*b*) CTIO/Las Campanas in V up to JD 2,446,890; (*c*) CTIO/Las Campanas in V from JD 2,446,891; and (*d*) ESO in Walraven V.

TABLE 1

SOURCES OF PHOTOMETRY AND POLARIMETRY FOR WR 47

Date (UT)	Telescope	Observer	Filters	Comparison Stars[a]
		Photometry		
1981 Aug 15–26	0.61 m CTIO	Cerruti (1984)	*UBV*	H2, H4
1985 Mar 25–Apr 11	0.61 m CTIO	RL	*V*	C2, C3
1987 Feb 8–24	1 m SAAO	CR	*R*	C2
1987 Mar 11–Apr 9	0.61 m CTIO	LD	*V*	C2, C3
1987 Apr 7–17	0.61 m LC	RL	*V*	C2, C3
1987 Apr 17–May 12	0.90 m ESO	NvW	Walraven[b]	C2, C3
		Linear Polarimetry		
1987 Feb 4–24	1 m SAAO[c]	CR	*R*	
1987 May 11–16	2.2 m ESO	AFJM/WS	*V*	
1987 Jun 22–25	2.15 m San Juan	VN/MC	*V*	
1988 Mar 16–26	2.15 m San Juan	VN/MC	*V*	

[a] H2, H4 from Feinstein and Marraco (1971); C2 = HD 110610, C3 = HD 110736.

[b] *V* at λ5403 (FWHM 708 Å), *B* λ4280 (423), *L* λ3840 (224), *U* λ3618 (234), and *W* λ3234 (157).

[c] With simultaneous circular polarization using the Cape Town polarimeter (Cropper 1985).

fairly noisy but clear phase-dependent modulation with amplitude $\sim$0.1 mag and sharp minimum at phase 0.070 ± 0.005. The previous 1981 data of Cerruti (1984) are compatible with this, although they are too sparse to provide a serious constraint.

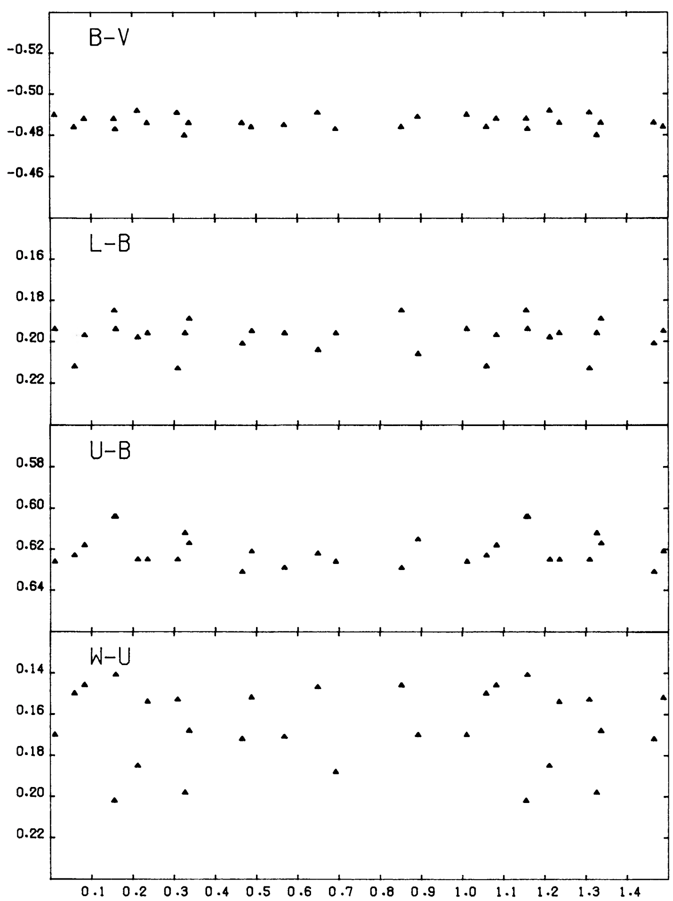

FIG. 2.—Walraven color indices of WR 47–C2 (here in magnitudes) vs. NM phase.

This phase shift differs slightly from all other well-observed WR + O systems, in which minimum light is observed to occur at zero phase (W-R star in front): cf. Moffat and Shara (1986) and Lamontagne and Moffat (1987). Thus, we assume that the NM period requires a small revision. Taking the NM *origin* of phases and requiring that the light curve minimum falls exactly at zero phase yields $P = 6^{\rm d}.2399 \pm 0^{\rm d}.0004$. Furthermore, an independent period search of the 1981–1987 photometric data alone yields $P = 6^{\rm d}.2395$, compared to the NM period of $6^{\rm d}.239 \pm 0^{\rm d}.003$. We therefore adopt the following ephemeris of zero phase (W-R star in front):

$$\text{JD } 2{,}443{,}918.4 + 6^{\rm d}.2399E\ .$$

All the photometric data are combined with this ephemeris in Figure 6, which shows a clear, sharp minimum at phase zero.

Note that the Walraven colors (Fig. 2) show no systematic correlation with phase (this is the case for C3 as well as for WR 47–C2) as do the magnitude variations, although the noise level does appear to be larger in some colors than in others. In particular, the *W* filter is most sensitive to emission-line flux because of the narrow bandpass close to the very strong line of He II 3203. This means that whatever is causing the systematic phase-dependent variation is essentially wavelength-independent, whereas the random continuum variations making the light curve appear noisy share the same random characteristics as the emission-line variations. Whether the

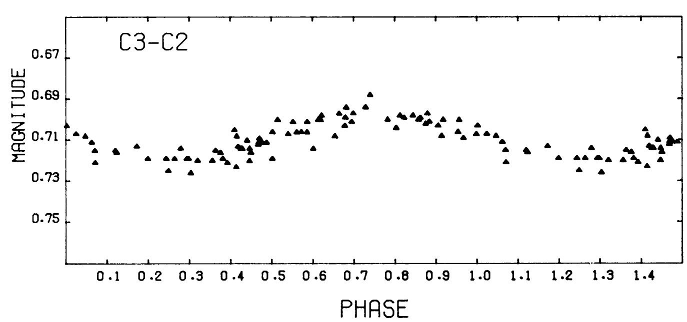

FIG. 3.—The 1987 *V* magnitudes of the comparison star differences C3–C2 vs. the phase of C3 (JD 2,446,149.6 + 1.68*E*; cf. Lamontagne and Moffat 1987).

TABLE 2A

1987 PHOTOMETRIC DATA

HJD-2,440,000	Orbital Phase[a]	WR 47 −C2	C3−C2	Source[b]
		R		
6834.610......	0.349	1.691	...	1
6840.612......	0.311	1.697	...	1
6841.580......	0.466	1.695	...	1
6845.447......	0.086	1.738	...	1
6845.550......	0.102	1.754	...	1
6847.556......	0.424	1.681	...	1
6848.517......	0.578	1.668	...	1
6849.466......	0.730	1.685	...	1
6850.542......	0.902	1.733	...	1
	mean	1.705		
	σ	0.030		
		V		
6865.817......	0.350	2.258	0.723	2
6867.832......	0.673	2.265	0.700	2
6869.724......	0.976	2.362	0.688	2
6869.795......	0.988	2.364	0.700	2
6870.671......	0.128	2.316	0.726	2
6870.772......	0.144	2.297	0.715	2
6870.850......	0.157	2.289	0.705	2
6871.681......	0.290	2.259	0.703	2
6871.786......	0.307	2.271	0.709	2
6873.729......	0.618	2.273	0.716	2
6873.811......	0.631	2.279	0.713	2
6874.695......	0.773	2.276	0.697	2
6875.671......	0.929	2.306	0.714	2
6875.739......	0.940	2.317	0.720	2
6875.799......	0.950	2.328	0.720	2
6875.842......	0.957	2.325	0.719	2
6880.660......	0.729	2.263	0.725	2
6880.743......	0.742	2.288	0.719	2
6881.658......	0.889	2.286	0.698	2
6881.776......	0.908	2.301	0.708	2
6881.844......	0.919	2.299	0.706	2
6882.640......	0.046	2.332	0.714	2
6882.708......	0.057	2.320	0.712	2
6882.765......	0.066	2.320	0.706	2
6882.830......	0.077	2.312	0.707	2
6882.884......	0.085	2.317	0.706	2
6883.643......	0.207	2.272	0.707	2
6883.804......	0.233	2.276	0.715	2
6884.645......	0.367	2.278	0.698	2
6884.743......	0.383	2.273	0.699	2
6884.825......	0.396	2.272	0.694	2
6885.691......	0.535	2.259	0.719	2
6885.774......	0.548	2.266	0.719	2
6886.645......	0.688	2.266	0.698	2
6886.750......	0.705	2.276	0.702	2
6886.822......	0.716	2.276	0.700	2
6887.659......	0.850	2.292	0.708	2
6887.752......	0.865	2.292	0.709	2
6887.826......	0.877	2.276	0.700	2
6888.746......	0.025	2.332	0.711	2
6889.651......	0.170	2.300	0.714	2
6889.757......	0.187	2.301	0.697	2
6889.808......	0.195	2.298	0.701	2
6891.702......	0.498	2.270	0.699	2
6891.805......	0.515	2.255	0.701	2
6892.722......	0.662	2.261	0.714	2
6892.790......	0.673	2.270	0.711	2
6894.596......	0.962	2.332	...	2
6894.738......	0.985	2.336	...	2
6894.770......	0.990	2.345	...	2
6894.786......	0.993	2.350	...	2
6894.820......	0.998	2.345	...	2
6894.866......	0.005	2.341	...	2
	mean	2.297	0.708	
	σ	0.030	0.009	
6892.716......	0.661	2.293	0.714	3
6892.822......	0.678	2.279	0.711	3
6893.761......	0.828	2.309	0.708	3
6894.624......	0.967	2.355	0.706	3
6894.721......	0.982	2.348	0.700	3
6894.826......	0.999	2.359	0.694	3
6895.696......	0.138	2.299	0.719	3
6895.805......	0.156	2.319	0.719	3
6896.709......	0.301	2.324	0.704	3
6896.808......	0.317	2.294	0.699	3
6897.746......	0.467	2.301	0.713	3
6897.842......	0.482	2.300	0.711	3
6898.718......	0.623	2.252	0.707	3
6898.839......	0.642	2.257	0.715	3
6899.706......	0.781	2.299	0.706	3
6899.820......	0.799	2.313	0.708	3
6902.713......	0.263	2.289	0.716	3
6902.822......	0.280	2.297	0.710	3
	mean	2.305	0.709	
	σ	0.029	0.007	
6902.741......	0.267	2.277	0.721	4
6903.688......	0.419	2.241	0.700	4
6904.690......	0.580	2.266	0.701	4
6907.872......	0.090	2.310	0.720	4
6908.806......	0.239	2.255	0.703	4
6909.788......	0.397	2.267	0.701	4
6913.639......	0.014	2.356	0.697	4
6914.593......	0.167	2.295	0.714	4
6916.661......	0.498	2.265	0.703	4
6918.686......	0.823	2.289	0.701	4
6919.725......	0.989	2.348	0.719	4
6920.681......	0.142	2.296	0.721	4
6923.681......	0.623	2.255	0.700	4
6924.678......	0.783	2.313	0.716	4
6925.670......	0.942	2.339	0.713	4
6926.569......	0.086	2.301	0.713	4
6927.635......	0.257	2.286	0.708	4
	mean	2.292	0.709	
	σ	0.033	0.009	

[a] From the ephemeris JD 2,443,918.4 + $6^{d}2399E$.

[b] (1) SAAO, (2) CTIO, (3) Las Campanas, (4) ESO.

NOTE.—The Walraven colors are from source (4) and are simultaneous with the preceding *V* data. The standard deviation for the *V* magnitudes of C3–C2 are reduced to $\sigma(o - c) \simeq 0.004$ mag after allowance for the light curve in Fig. 3.

TABLE 2B

(WR 47–C2)				(C3–C2)				
	$B-V$	$L-B$	$U-B$	$W-U$	$B-V$	$L-B$	$U-B$	$W-U$
	−0.486	+0.189	+0.617	+0.168	+0.245	+0.318	+0.521	+0.298
	−0.484	+0.189	+0.621	+0.152	+0.246	+0.306	+0.524	+0.320
	−0.491	+0.204	+0.621	+0.146	+0.234	+0.321	+0.522	+0.305
	−0.483	+0.194	+0.604	+0.141	+0.242	+0.316	+0.528	+0.330
	−0.491	+0.213	+0.625	+0.153	+0.239	+0.305	+0.514	+0.321
	−0.486	+0.201	+0.631	+0.172	+0.244	+0.301	+0.514	+0.320
	−0.488	+0.197	+0.618	+0.146	+0.239	+0.310	+0.523	+0.310
	−0.486	+0.196	+0.625	+0.154	+0.236	+0.320	+0.515	+0.328
	−0.482	+0.196	+0.629	+0.171	+0.239	+0.313	+0.520	+0.315
	−0.489	+0.206	+0.615	+0.169	+0.236	+0.309	+0.522	+0.310
	−0.485	+0.212	+0.623	+0.150	+0.241	+0.310	+0.533	+0.317
	−0.492	+0.198	+0.626	+0.185	+0.241	+0.302	+0.516	+0.341
	−0.483	+0.196	+0.626	+0.187	+0.235	+0.309	+0.524	+0.306
	−0.484	+0.185	+0.629	+0.147	+0.240	+0.305	+0.522	+0.316
	−0.490	+0.195	+0.625	+0.170	+0.245	+0.308	+0.511	+0.327
	−0.488	+0.185	+0.604	+0.202	+0.242	+0.304	+0.515	+0.330
	−0.480	+0.196	+0.612	+0.197	+0.240	+0.302	+0.518	+0.301
mean	−0.486	+0.198	+0.621	+0.165	+0.240	+0.309	+0.520	+0.317
σ	0.004	0.008	0.008	0.019	0.004	0.006	0.006	0.012

source of continuum and line variations are related to the same wind variability (e.g., blob ejection: cf. Moffat *et al.* 1988) remains to be shown. On the other hand, WR 47 is about 2 mag fainter than either C2 or C3, so that the increased noise as one goes farther out into the UV in Table 2 may be instrumental in origin.

Because of the wavelength-independence of the phase-dependent variations, we can assume that electron scattering is likely at work here. *The fact that light minimum occurs close to zero phase strongly suggests that these light variations are due to phase-dependent transparency variations of O-star light as the companion O star orbits in the hot W-R star wind*, where free electrons abound. Also, there is no obvious second dip in the light curve at phase 0.5 as would be expected if we were dealing with actual eclipses between the two hot stars in a circular orbit.

A more detailed yet simple model for the general trend of the light curve in Figure 6 bears out the above hypothesis. We start by writing an expression for the magnitude difference W-R minus comparison star for single scattering:

$$\Delta m = \text{const} - 2.5 \log (I_{\text{W-R}} + I_{\text{O}} e^{-\tau}) , \tag{1}$$

where $I_{\text{W-R}}$ and I_{O} refer to the intrinsic intensity (assumed constant with time) for each star and τ is the free electron optical depth from the O star through the W-R star wind along the line of sight to the observer. Taking the O star as a point source (justification follows below), an element of optical depth can be written as

$$d\tau = \sigma_e n_e dz , \tag{2}$$

where σ_e is the Thomson scattering coefficient for a nonrelativistic electron (6.65×10^{-25} cm^2), n_e is the electron density, and z is the distance along the line of sight, starting from the W-R star ($z = 0$). Further development of equation (2) is as follows. We take $n_e = \alpha\rho/m_p$, where α is the number of electrons per baryon mass m_p; (e.g., $\alpha = 0.5$ for 100% He^{++}), and ρ is the total wind density. Also, we have the mass flux conservation equation $\dot{M} = 4\pi r^2 \rho(r) v(r)$, in which the (radial) wind velocity law can be parameterized as $v(r) = v_\infty(1 - R_*/r)^\beta$, where R_* is the core radius of the W-R star, v_∞ is the terminal wind speed, and β is a form parameter (usually $0.5 \lesssim \beta \lesssim 1.0$; the observed velocity law for the W-R component in the eclipsing WN5+O6 binary V444 Cygni bears this out with some preference for a value at the higher end of the range: Cherepashchuk, Eaton, and Khaliullin 1984).

For a circular orbit with the W-R star arbitrarily taken to be at the origin, the O star will have coordinates

$$x_0 = -(a \cos i) \cos 2\pi\phi$$
$$y_0 = -a \sin 2\pi\phi$$
$$z_0 = -(a \sin i) \cos 2\pi\phi ,$$

where x_0, y_0 are measured in the plane of the sky with y_0 coinciding with the line of nodes, and a, i, and ϕ are the orbital separation, inclination, and phase, respectively. Thus, we obtain

$$\tau = \int_{z=z_0}^{\infty} d\tau = k \int_{-\sin i \cos 2\pi\phi}^{\infty} \frac{du}{(r/a)^2(1 - R_*/r)^\beta} \tag{3}$$

in which

$$u = z/a, \quad r^2 = x_0^{\,2} + y_0^{\,2} + z_0^{\,2} ,$$
$$(r/a)^2 = (\cos^2 i \cos^2 2\pi\phi + \sin^2 2\pi\phi) + u^2 ,$$

and the constant

$$k = \frac{\alpha\sigma_e \dot{M}}{4\pi m_p v_\infty a} = 0.048 \frac{(2\alpha)(\dot{M}/5 \times 10^{-5}\ M_\odot\ \text{yr}^{-1})}{(v_\infty/3000\ \text{km s}^{-1}) \times (a/50\ R_\odot)} .$$

The integral in equation (3) is a dimensionless quantity which varies with phase; it is integrable in closed form only for $\beta = 0$; i.e., $v = v_\infty$. We started by integrating equation (3) numerically for a range of reasonable values of β(0.0–1.0), R_*(3–7 $R_\odot$), $I_{\text{O}}/I_{\text{W-R}}$(0.2–1.5), and i(60°–80°), fitting to each photometric data set. For a given value of i, the shape of the fitted curves varied insignificantly for different values of β, R_*, and $I_{\text{O}}/I_{\text{W-R}}$ in the above ranges. Thus, in Table 4 we present only the value of i which yields the best fit for each data set. A simple mean gives $i_{\text{phot}} = 63° \pm 7°$. This value overlaps with the best value from the polarization data ($i_{\text{pol}} = 73° \pm 5°$; see below). We adopt a weighted mean $i = 70° \pm 4°$. Note that the least noisy light curve [1987(2) in Table 4] yields $i = 71°$, the closest photometric inclination to the adopted value.

TABLE 3

LINEAR AND CIRCULAR POLARIZATION DATA

JD (−2,440,000)	Orbital Phase[a]	P (%)	σ_p (%)	θ	σ_θ	V (%)	σ_V (%)	Source[b]
6830.613	0.708	3.761	0.037	64°.9	0°.3	-	-	1
6834.610	0.349	4.047	0.054	65.1	0.4	+0.057	0.035	1
6840.612	0.311	3.813	0.054	64.6	0.4	−0.076	0.034	1
6841.594	0.468	4.360	0.054	66.4	0.4	+0.020	0.027	1
6843.529	0.778	3.878	0.053	67.9	0.4	−0.065	0.035	1
6844.510	0.935	4.207	0.058	65.1	0.4	+0.084	0.037	1
6845.447	0.086	4.043	0.067	60.7	0.5	−0.073	0.033	1
6845.550	0.102	4.036	0.062	61.9	0.4	−0.034	0.032	1
6846.500	0.254	3.686	0.061	64.9	0.5	+0.049	0.031	1
6847.556	0.424	4.265	0.061	63.7	0.4	-	-	1
6848.517	0.578	4.055	0.054	63.8	0.4	−0.029	0.029	1
6849.466	0.730	3.810	0.055	64.5	0.4	−0.043	0.026	1
6850.542	0.902	4.233	0.054	64.6	0.4	−0.081	0.034	1
6926.638	0.097	4.390	0.022	68.6	0.1	-	-	2
6927.646	0.259	3.977	0.028	69.2	0.2	-	-	2
6928.829	0.448	4.652	0.061	69.1	0.4	-	-	2
6929.663	0.582	4.341	0.022	68.0	0.2	-	-	2
6930.656	0.741	3.953	0.022	69.5	0.2	-	-	2
6931.787	0.922	4.531	0.028	69.4	0.2	-	-	2
6969.625	0.986	4.381	0.032	66.2	0.2	-	-	3
6971.603	0.303	3.931	0.029	69.6	0.2	-	-	3
6972.599	0.463	4.410	0.034	68.1	0.2	-	-	3
7236.850	0.811	4.003	0.032	69.2	0.2	-	-	4
7237.696	0.947	4.318	0.037	69.4	0.2	-	-	4
7238.732	0.113	4.111	0.025	66.5	0.2	-	-	4
7239.753	0.227	3.856	0.028	69.8	0.2	-	-	4
7240.694	0.427	4.409	0.022	69.0	0.1	-	-	4
7242.752	0.757	3.956	0.025	69.1	0.2	-	-	4
7243.681	0.906	4.318	0.028	68.2	0.2	-	-	4
7244.724	0.073	4.235	0.030	66.8	0.2	-	-	4
7245.719	0.233	3.896	0.026	68.5	0.2	-	-	4
7246.711	0.392	4.250	0.025	69.2	0.2	-	-	4

[a] The orbital phase was calculated with the ephemeris: JD 2,443,918.4 + 6.2399*E*.
[b] (1) 1987, SAAO; (2) 1987, ESO; (3) 1987, San Juan; (4) 1988, San Juan (see Table 1).

With $i = 70°$ and the above range of the parameters β, R_*, and $I_O/I_{W\text{-}R}$, it can be shown that $\tau \ll 1$. Thus equation (1) can be simplified for the optically thin case:

$$\Delta m \simeq \text{const} + 0.43 f_c \tau \,, \tag{4}$$

TABLE 4

BEST VALUES OF THE ORBITAL INCLINATION FROM THE PHOTOMETRY

Source[a]	i(°)[b]
1985	77
1987 (2)	71
1987 (3)	47
1987 (4)	58
mean	63° ± 7°
σ	13°

[a] Cf. Table 1 (The 1981 and 1987 [1] data are too sparse to provide useful constraints here).
[b] Calculated for $\beta = 1$, $R_* = 5\ R_\odot$, although these values of i are nearly independent of any reasonable values for β and R_*.

where f_c is the intensity of the O-type companion relative to the total light, i.e.,

$$f_c = I_O/(I_{W\text{-}R} + I_O) \,.$$

Now, fitting equations (3) and (4) (cf. Fig. 7) yields

$$f_c\, k\ (\text{phot}) = 0.009 \,, \tag{5}$$

independent of β and R_* in the range given above (we actually take the most likely values of $\beta \simeq 1$ and $R_* \simeq 5R_\odot$).

At this point it is appropriate to note that allowance for a realistic, finite disk along with limb darkening for the O star has no significant effect on the above result. Figure 8 compares the calculated light curve using the point source approximation of equations (3) and (4) above, with a projected disk of an O5 V star of radius $R_O = 12\ R_\odot$ (Schmidt-Kaler 1982) and limb darkening function for hot stars $J = 0.4 + 0.6 \cos \gamma$, where γ is the angle between the radius vector on the star and the observer (Kopal 1959). This was done for $\beta = 0$, for which the calculations are the least time consuming. Since the point source approximation is little affected by using larger values of β (≤ 1), it is not expected that the finite limb-darkened disk calculations will be changed either, for larger β.

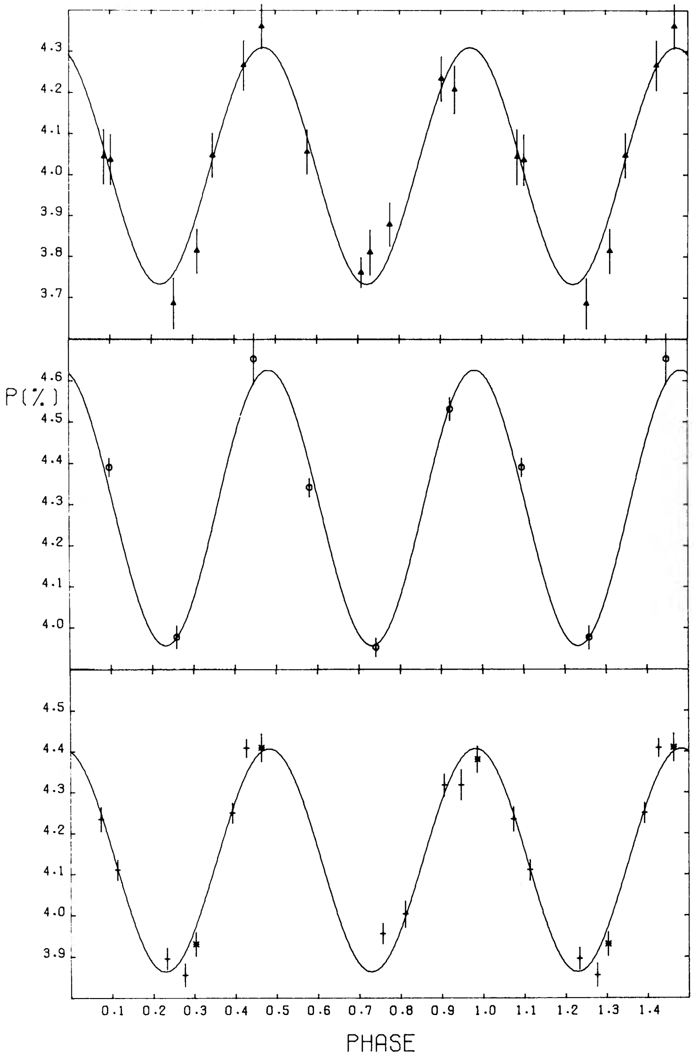

FIG. 4a

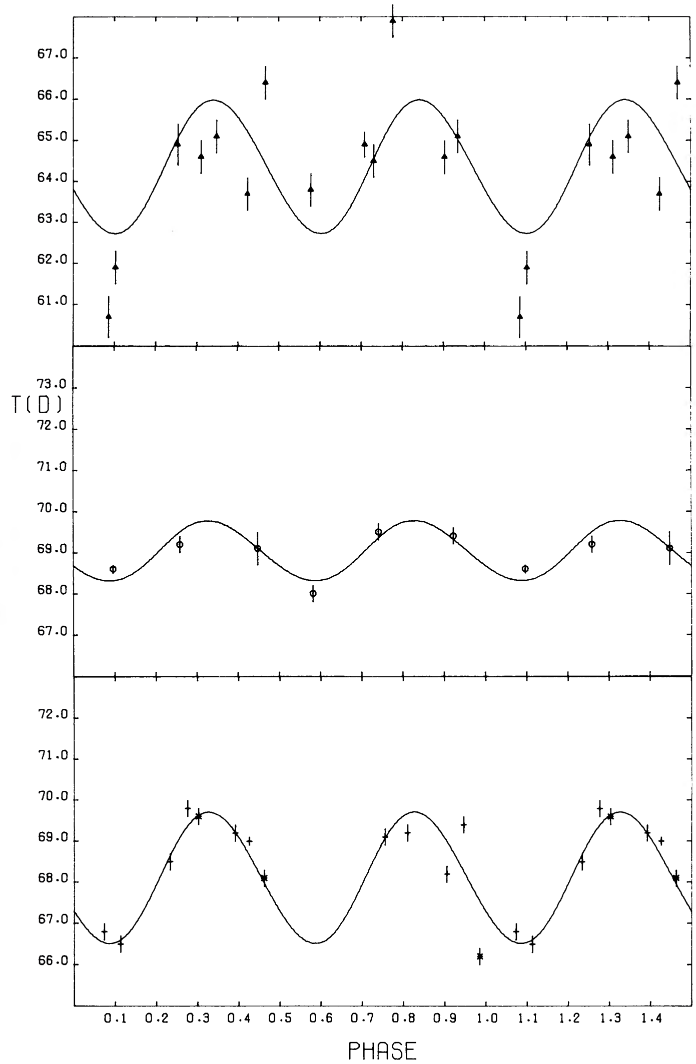

FIG. 4b

FIG. 4.—The linear polarization data (*a*) *P* and (*b*) θ, vs. the revised phase of this paper. From top to bottom: (i) SAAO in *R*, (ii) ESO in *V*, and (iii) San Juan in *V*. The curves are based on a second harmonic fit in *Q*, *U*. Error bars are 2 σ estimates (cf. Table 3). The different symbols in (iii) refer to two different epochs.

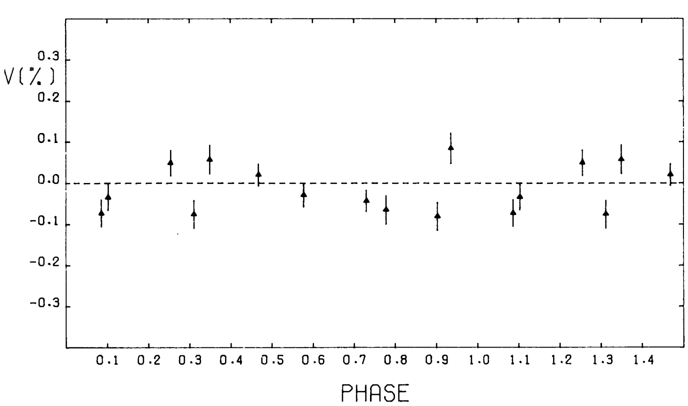

FIG. 5.—Circular polarization versus the revised phase of this paper, simultaneous with the linear polarization data in Fig. 4 (i).

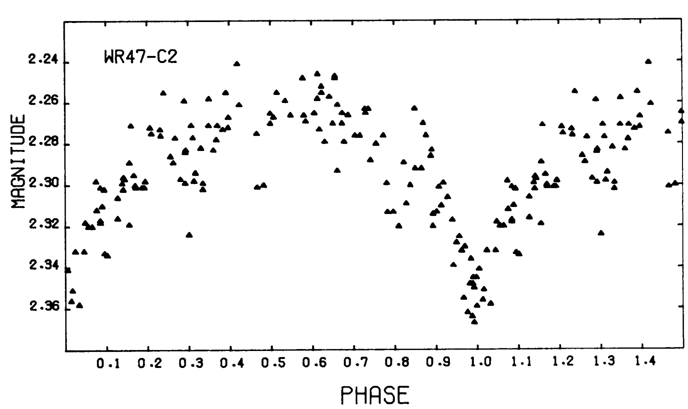

FIG. 6.—All the photometric data (1981–1987) after shifting each set in magnitude and using the revised phase of this paper.

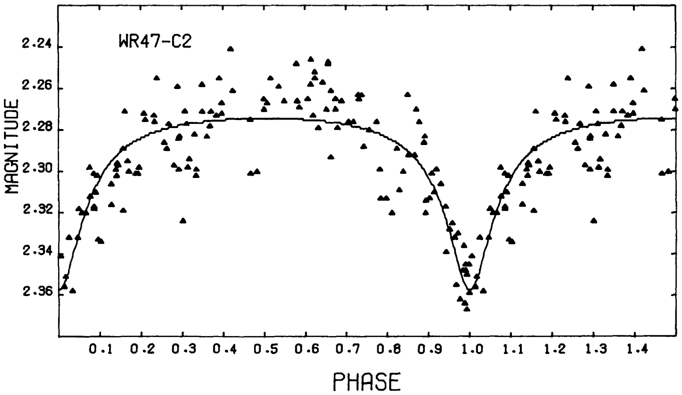

FIG. 7.—Best fit to the photometric data of Fig. 6 with $i = 70°$, $\beta = 1$, $R_* = 5\ R_\odot$, and $f_c\, k = 0.0095$.

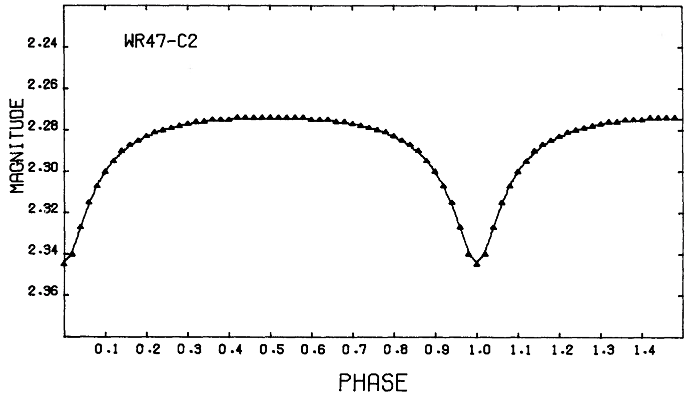

FIG. 8.—Comparison of the model light curve for $\beta = 0$ without (*full curve*) and with (*points*) limb darkening of a finite disk of $R = 12\ R_\odot$.

We also note the minimum *projected* separation between the stars $a \cos i = 23.3\ R_\odot$ (based on $a \sin i = 64\ R_\odot$; cf. NCM). For $R_{\text{W-R}} = 5 \pm 2\ R_\odot$ and $R_{\text{O}} = 12\ R_\odot$, we get $R_{\text{W-R}} + R_{\text{O}} \simeq 17 \pm 2\ R_\odot$. Since $R_{\text{O}} + R_{\text{W-R}}$ is less than $a \cos i$, it is understandable that the observed light curve does not show even partial eclipses of the stars (no minimum at phase 0.5); rather, only strong transparency effects by the W-R wind are apparent, as already suspected at the outset.

b) Polarimetry

Since the linear polarization data in Figure 4 show a clear double wave per orbit, we forced a *second* harmonic fit in $Q(\equiv P \cos 2\theta)$ and $U(\equiv P \sin 2\theta)$ to each of the three data sets, according to the theory of Brown, McLean, and Emslie (1978): $Q = q_0 + q_3 \cos 4\pi\Phi + q_4 \sin 4\pi\Phi$, $U = u_0 + u_3 \cos 4\pi\Phi + u_4 \sin 4\pi\Phi$, where Φ is the orbital phase. The fitted parameters are listed in Table 5 and determine the curves in Fig. 4. The estimated errors of the fit appear to be about a factor 2 smaller than the scatter among the three sources. This may be due to the erratic variability of the star or possibly to systematic errors, which are difficult to assess. In any case, we take the three sources at face value and derive the weighted mean inclination $i = 107° \pm 5°$ (or $73° \pm 5°$, when referred to radial velocity orbits which cannot distinguish between prograde and retrograde motion), and mean semi-major axis of the Q-U plane ellipse, $A_p = 0.26\%$. Again, we note that the amplitudes in the bandpasses V and R are identical within the errors, as expected for wavelength-independent electron scattering.

The circular polarization plotted in Figure 5 shows no correlation with phase as expected in the case of polarization via electron scattering (cf. Robert and Moffat 1989). The mean is $V = -0.017\% \pm 0.018\%$. The scatter, $\sigma_v = 0.060\%$, is again significantly larger than the estimated errors (rms 0.032%).

The value of $i(70°)$ can now be combined with the orbital masses ($M \sin^3 i$) of NCM to obtain the actual masses:

$$M_{\text{WN6}} = \frac{40\ M_\odot}{0.83} = 48 \pm 5\ M_\odot$$

$$M_{\text{O5: V}} = \frac{47\ M_\odot}{0.83} = 57 \pm 6\ M_\odot\ ,$$

with uncertainties based on the propagation of independent errors in K_{WR}, K_{O}, i, and P. Not only is this the highest mass W-R star known (neglecting the less certain systems HD 92740 and HD 193077; cf. Smith and Maeder 1989), but the O-star is also one of the most massive known. In fact, it may be easier to obtain masses of early O-stars in W-R + O binaries than in O + O binaries, due to the clearer separation of the two sets of spectral lines in W-R + O systems.

Following the work on polarization of W-R binaries of St-Louis *et al.* (1988), A_p and i can be used to estimate the mass-loss rate, assuming a spherically symmetric wind

$$A_p = \frac{2\alpha(1 + \cos^2 i)3\sigma_e f_c \dot{M}}{(16\pi)^2 m_p v_\infty a} I\ , \tag{6}$$

where I is a dimensionless integral that depends on the wind velocity law and the polarization geometry. St-Louis *et al.* (1988) give $I = 5.7$ for WR 47 based on $\beta = 0.5$, $\epsilon \approx 2$, and the ESO polarimetry only. (ϵ gives the fractional stellar radius where the wind changes from being optically thick to thin.) Here, we take the asymptotic limit $I = 7.75$ which is better suited for $\beta \approx 1$, $\epsilon \approx 2$. Thus, equation (6) yields

$$f_c\, k(\text{pol}) = \frac{32\pi A_p}{3(1 + \cos^2 i)I} = 0.010\ . \tag{7}$$

It is encouraging to note that both the photometry and polarimetry yield similar values of $f_c\, k$. This is not just a coincidence, even though the basic physical process is the same, i.e., electron scattering. Indeed, the geometry of the column density

TABLE 5

PARAMETERS FROM THE SECOND HARMONIC FIT IN LINEAR POLARIZATION

Parameter	SAAO R	ESO V	San Juan V
q_0 (%)	-2.514 ± 0.013	-3.191 ± 0.012	-2.982 ± 0.007
u_0 (%)	$+3.137 \pm 0.013$	$+2.869 \pm 0.012$	$+2.865 \pm 0.007$
q_3 (%)	-0.105 ± 0.018	-0.205 ± 0.015	-0.107 ± 0.009
u_3 (%)	$+0.262 \pm 0.018$	$+0.260 \pm 0.015$	$+0.271 \pm 0.009$
q_4 (%)	$+0.230 \pm 0.019$	$+0.118 \pm 0.017$	$+0.183 \pm 0.009$
u_4 (%)	$+0.054 \pm 0.019$	$+0.021 \pm 0.017$	$+0.097 \pm 0.009$
i (°)	119 ± 6	99 ± 2	114 ± 2
Ω (°)	-52 ± 13	-48 ± 3	-75 ± 4
$10^3\, \tau_0 \gamma_3$	2.2 ± 0.3	3.2 ± 0.2	2.5 ± 0.1
$10^3\, \tau_0 \gamma_4$	0.8 ± 0.5	0.6 ± 0.2	-0.4 ± 0.2
λ_2 (°)	10 ± 6	5 ± 2	-4 ± 2
$\sigma_{o-c}(Q)$ (%)	0.17	0.07	0.05
$\sigma_{o-c}(U)$ (%)	0.12	0.02	0.06

for the light curve refers to a more localized region compared to the more global distribution of the polarization scattering material.

Taking an overall mean solution of $f_c k = 0.0095$ along with the parameters $v_\infty = 3320$ km s^{-1} (Abbott and Conti 1987), $a = 68\ R_\odot$, $\alpha = 0.5$, and $f_c \approx 0.5$ (both stars of the same absolute magnitude), we get

$$\dot{M} = \frac{4\pi m_p v_\infty a}{\alpha \sigma_e f_c} (f_c k) = 3 \times 10^{-5}\ M_\odot\ \mathrm{yr}^{-1} .$$

The least certain factors here are α and f_c. If the wind consists of 100% He^+ (less likely than He^{++}) one would have $\alpha = 0.25$ and $\dot{M}$ twice as large. The value of f_c is based on the mean of M_v (O5 V) $= -5.7$ (Schmidt-Kaler 1982) and -5.5 (Humphreys and McElroy 1984) and the mean for WN6 ($M_v = -5.2$) and WN7 ($M_v = -6.5$) from Lundström and Stenholm (1984); cf. also van der Hucht *et al.* (1988). As a member of the open cluster Hogg 15 (Moffat 1974), WR 47 would have a total magnitude $M_v = -5.9$, compatible with the spectroscopic values of M_v within the errors, typically 0.5 mag per star. Furthemore, if the value of v_∞ of W-R stars in general has to be decreased by $\sim 30\%$ (Williams and Eenens 1989), this will decrease $\dot{M}$ by the same amount.

IV. SUMMARY AND CONCLUSIONS

WR 47 shows phase-dependent modulation in light and in linear polarization that can both be explained in a consistent way on the basis of electron scattering of O-star light in a spherically symmetric wind from the W-R component. Major perturbations by the much more tenuous wind of the early O-type main-sequence companion (cf. Shore and Brown 1988 for V444 Cygni) are not evident. Thus, our understanding of the global properties of hot, dense stellar winds of W-R stars cannot be too far off base.

Detailed analysis leads to an orbital inclination $i = 70° \pm 4°$ and a mass-loss rate $\dot{M}$(W-R) $= 3 \times 10^{-5}\ M_\odot$ yr^{-1}, a value that is compatible with determinations using other methods (cf. Abbott *et al.* 1986 for radio data).

The masses of both components of WR 47 are very high: 48 $M_\odot$ for the WN6 star and 57 $M_\odot$ for the O star. The next highest fairly reliable mass for a WNL star is 46: $M_\odot$ for CQ Cep (cf. Leung, Moffat, and Seggewiss 1983), although this is a WN7 star (less evolved than WN6?) with a *less* massive O companion. (This could change if indeed Lipunova and Cherepashchuk [1982], Niemela [1982], and Kartasheva and Snezhko [1985] have really detected the absorption orbit of the O companion in CQ Cep). Presumably we are seeing the beginning phase of the evolution of the originally more massive component into the W-R phase of very rapid mass loss. If the present rate of mass loss is retained or (more likely) even increased with time, the W-R component could halve its *present* mass in $\lesssim 8.10^5$ yr and arrive in the domain of the WNE or WC stars, before its final fate either exploding as a supernova or shrinking into a stable low-mass He star.

A. F. J. M. is grateful to the Canadian NSERC for financial support. V. S. N. and M. A. C. would like to express their gratitude for the use of the CASLEO facilities in San Juan, and thank the Vatican Observatory for the loan of their polarimeter.

REFERENCES

Abbott, D. C., Bieging, J. H., Churchwell, E., and Torres, A. V. 1986, *Ap. J.*, **303**, 239.
Abbott, D. C., and Conti, P. S. 1987, *Ann. Rev. Astr. Ap.*, **25**, 113.
Brown, J. C., McLean, I. S., and Emslie, A. G. 1978, *Astr. Ap.*, **68**, 415.
Cerruti, M. A. 1984, *Info. Bull. Var. Stars*, No. 2637.
Cherepashchuk, A. M., Eaton, J. A., and Khaliullin, K. F. 1984, *Ap. J.*, **281**, 774.
Conti, P. S. 1976, *Mem. Soc. Roy. Sci. Liège*, ser. 6, **9**, 193.
Cropper, M. 1985, *M.N.R.A.S.*, **212**, 709.
Dolan, J. F., and Tapia, S. 1988, *Astr. Ap.*, **202**, 124.
Feinstein, A., and Marraco, H. G. 1971, *Pub. A.S.P.*, **83**, 218.
Humphreys, R. M., and McElroy, D. B. 1984, *Ap. J.*, **284**, 565.
Karasheva, T. A., and Snezhko, L. I. 1985, *Soviet Astr.*, **29**, 440.
Kopal, Z. 1959, *Close Binary Systems* (London: Chapman-Hall), p. 153.
Lamontagne, R., and Moffat, A. F. J. 1987, *A.J.*, **94**, 1008.
Leung, K.-C., Moffat, A. F. J., and Seggewiss, W. 1983, *Ap. J.*, **265**, 961.
Lipunova, N. A. amd Cherepashchuk, A. M. 1982, *Soviet Astr.*, **26**, 569.
Lundström, I., and Stenholm, B. 1984, *Astr. Ap. Suppl.*, **58**, 163.
Moffat, A. F. J. 1974, *Astr. Ap.*, **34**, 29.
Moffat, A. F. J. 1981, in *IAU Colloquium 59, Effects of Mass Loss on Stellar Evolution*, ed. C. Chiosi and R. Stalio (Dordrecht: Reidel), p. 301.
———. 1982, in *IAU Symposium 99, Wolf-Rayet Stars: Observations, Physics, Evolution*, ed. C. W. H. de Loore and A. J. Willis (Dordrecht: Reidel), p. 515.
Moffat, A. F. J., Drissen, L., Lamontagne, R., and Robert, C. 1988, *Ap. J.*, **334**, 1038.
Moffat, A. F. J., and Seggewiss, E. 1987, *ESO Messenger*, No. 49, 26.
Moffat, A. F. J., and Shara, M. M. 1986, *A.J.*, **92**, 952.
Niemela, V. S. 1982, in *IAU Symposium 88, Close Binary Stars: Observations and Interpretation*, ed. M. J. Plavec, D. M. Popper, and R. K. Ulrich (Dordrecht: Reidel), p. 177.
Niemela, V. S., Conti, P. S., and Massey, P. 1980, *Ap. J.*, **241**, 1050 (NCM).
Niemela, V. S., and Mandrini, C. H. 1989, in preparation (NM).
Robert, C., and Moffat, A. F. J. 1989, *Ap. J.*, **343**, 902.
St-Louis, N., Moffat, A. F. J., Drissen, L., Bastien, P., and Robert, C. 1988, *Ap. J.*, **330**, 286.
Schmidt-Kaler, Th. 1982, in *Landolt-Börnstein*, New Ser., Group 6, Vol. 26, ed. K. H. Hellwege (Berlin: Springer-Verlag), p. 1.
Shore, S. N., and Brown, D. N. 1988, *Ap. J.*, **324**, 1021.
Smith, L. F., and Maeder, A. 1989, *Astr. Ap.*, **211**, 71.
van der Hucht, K. A., Hidayat, B., Admiranto, A. G., Supelli, K. R., and Doom, C. 1988, *Astr. Ap.*, **199**, 217.
van der Hucht, K. A., Conti, P. S., Lundström, I., and Stenholm, B. 1981, *Space Sci. Rev.*, **28**, 227.
Williams, P. M., and Eenens, P. R. J. 1989, in *IAU Colloquium 113, Physics of Luminous Blue Variables*, ed. K. Davidson, A. F. J. Moffat and H. J. G. L. M. Lamers (Dordrecht: Kluwer), p. 308.

Note added in proof.—Subsequent search of integral tables shows that equation (3) is integrable in closed forms also for $\beta = 1$ and 2.

M. A. Cerruti and V. S. Niemela: Instituto de Astronomia y Fisica del Espacio, Casilla de Correo 67, Suc. 28, 1428 Buenos Aires, Argentina

R. Coziol, L. Drissen, R. Lamontagne, A. F. J. Moffat, N. Mousseau, and C. Robert: Département de physique, Université de Montréal, C.P. 6128, Succ. A, Montréal, PQ, Canada H3C 3J7

W. Seggewiss: Observatorium Hoher List, 5568 Daun, F.R. Germany

N. van Weeren: Leiden Observatory, Postbus 9513, NL-2300 RA Leiden, The Netherlands